Revised

REGULATION OF THE ARYL HYDROCARBON RECEPTOR ACTIVITY IN BOVINE CUMULUS-OOCYTE COMPLEXES DURING *IN VITRO* MATURATION: THE ROLE OF EGFR AND POST-EGFR ERK1/2 SIGNALING CASCADE

Paola Pocar[1, 3], Anna Berrini[1], Alessia Di Giancamillo[1], Bernd Fischer[2], Vitaliano Borromeo[1]

[1]Department of Veterinary Medicine, University of Milano, I-20133 Milano (Italy)

[2]Department of Anatomy and Cell Biology, Martin Luther University, Faculty of Medicine, D-06097 Halle (Saale), Germany

Running title: AhR regulation in cumulus-oocyte complexes

[3] To whom correspondence should be addressed at:
Department of Veterinary Medicine
Via Celoria 10
I-20133 Milano (Italy)
Tel + 39 02 50318125, Fax + 39 02 50318123
paola.pocar@unimi.it

ABSTRACT

The aryl hydrocarbon receptor (AhR) has been extensively characterized as an environmental sensor with major roles in xenobiotic-induced toxicity. Evidence is accumulating that these functions serve as adaptive mechanisms overlapping its physiological roles. We previously described a critical role of constitutive AhR activation for the correct progress of mammalian oocyte maturation but the signaling pathway through which AhR controls maturation remains unclear.

The aim of this study was to investigate whether the AhR interacts with the epidermal growth factor receptor (EGFR) and p42/44 extracellular regulated kinases (ERK1/2), both key factors in the signaling network that finely regulates the oocyte maturation. As experimental model we used bovine cumulus-oocyte complexes (COCs) during *in vitro* maturation (IVM).

Blocking ERK1/2 signaling in COCs during IVM with the specific EGFR inhibitor AG1478 or the mitogen-activated protein kinase kinase (MEK) inhibitor PD98059 downregulated the expression of the AhR-target gene Cyp1a1. Inhibition of AhR activity was associated with a reduction in the oocytes' ability to progress in meiosis resumption. In contrast, exposure to the AhR antagonist resveratrol reduced both *CYP1A1* expression and the oocytes' maturation competence, without affecting ERK1/2 signaling.

These findings strongly indicate the EGFR/ERKs signaling network as an upstream regulator of the AhR activation in COCs, offering a new understanding of the finely tuned physiological mechanism leading to oocyte maturation. This information may provide fresh opportunities for improving oocyte *in vitro* maturation, and therefore boosting the efficiency of assisted reproduction techniques in mammals.

45 Key words: Aryl hydrocarbon receptor (AhR), cytochrome p450 1A1 (*CYP1A1*), cumulus-
46 oocyte complex (COC), *in vitro* maturation, 42/44 extracellular regulated kinases (ERK 1/2),
47 epidermal growth factor receptor (EGFR)
48

1. INTRODUCTION

Female fertility relies on proper maturation of the oocyte. Oocyte maturation is a highly complex cellular process involving the meiotic cell cycle progression and cytoplasmic changes that determines the subsequent successful fertilization, zygote formation, attainment of blastocyst stage, normal embryo growth and development, as well as appropriate implantation [1-3]. In mammals, the molecular machinery governing oocyte maturation is controlled by multiple interactions among different signaling pathways [4, 5]. Despite significant advances the molecular mechanisms underpinning the process of oocyte maturation, yet many key questions remain to be resolved.

In this context, we previously reported that the aryl hydrocarbon receptor (AhR) is constitutively activated in mammalian cumulus-oocyte complexes (COCs) during *in vitro* maturation (IVM), as shown by the upregulation of the two main target genes *CYP1A1* and *CYP1B1* in the absence of exogenous ligands [6, 7]. In addition, AhR activation appears to be necessary for correct progressing of meiosis resumption, since treatment with specific AhR antagonists during IVM negatively affects the oocytes' ability to reach the metaphase II [7]. The molecular mechanisms by which AhR exerts its effect in the mammalian cumulus-oocyte complex are still not understood.

The AhR is a ligand-activated transcription factor of the basic helix-loop-helix/per-ARNT-Sim (bHLH/PAS) superfamily. Since the early 1990's, the AhR has been defined as an environmental sensor with major roles in xenobiotic-induced toxicity and carcinogenicity [8]. The AhR can in fact be activated by planar aromatic hydrocarbons such as 2,3,7,8-tetrachlorodibenzo-p-dioxin (TCDD), benzo[a]pyrene (B[a]P), dibenzofurans and planar polychlorinated biphenyls (PCBs), all of which are widely detectable in the environment [9, 10].

In its resting state AhR is sequestered in the cytosol in a multiprotein complex with heat shock protein 90 (hsp90), p23 and the AhR interacting protein (AIP) [11]. Upon ligand binding, AhR translocates into the nucleus where it forms a heterodimer with the AhR nuclear translocator (ARNT). The AhR/ARNT complex then binds to a specific DNA sequence (xenobiotic responsive element - XRE) in the promoter of target genes and triggers their expression. The AhR gene battery consists of genes encoding for phase I and II drug metabolizing enzymes, with cytochrome P450 (CYP) 1A1 as the main one, as well as for proteins involved in regulating cell growth and differentiation [9, 11, 12].

The view that the AhR is exclusively a promiscuous cytosolic sensor of xenobiotic chemicals is changing. Evidence is accumulating that xenobiotic-dependent AhR functions are an adaptive mechanism, overlapping its physiological roles. In fact, a significant number of studies support its contribution to the proper functioning of the immune, hepatic, cardiovascular and reproductive systems [13-16]. However, little is known about its physiological function and its endogenous ligands.

To date, a number of putative endogenous AhR-activating factors have been identified [17-19]. However, the physiological consequences of AhR activation by these ligands still need to be elucidated. AhR-dependent transcriptional activity is both ligand- and cell-specific. For a given cell type, it may even depend on the tissue milieu, such as in an ongoing immune response [20, 21]. Furthermore, gene microarray studies have reported that different AhR ligands can induce a distinctly different, ligand-specific set of gene products [22, 23].

Activated AhR signaling impinges on numerous molecular pathways in eukaryotic cells [24]. There is strong evidence of two-way cross-talk between AhR and the RAS-RAF-MEK-ERK1/2 pathway which is the most important pathway mediating the biological response of the epidermal growth factor receptor (EGFR-ErbB1) [25].

In bovine COCs, EGFR and ERKs are both key factors in coordinating oocyte maturation. Their activation is necessary for gonadotropin-induced oocyte meiotic resumption, regulation of microtubule organization and meiotic spindle assembly [26, 27] and for the maintenance of metaphase II arrest [28, 29]. Given the proven interactions between AhR and the RAS-RAF-MEK-ERK1/2 pathway and the central role of EGFR/ERKs in COCs, it is logical to hypothesize that AhR might interact with ERKs and EGFR in the complex signaling network regulating the progression of mammalian oocyte maturation. We set out to find proof of this cross-talk in bovine COCs during IVM. The COC is a morpho-functional unit and the relationship between the two compartments allow for important physiological processes such as oocyte growth, meiotic resumption, maintenance of meiotic arrest and acquisition of developmental competence. In previous studies, we showed that *CYP1A1* expression pattern was similar in oocytes and cumulus cells during IVM (Pocar et al., 2004), thus in the present study we elicited to consider the entire COC as physiological entity.

Clarifying the biological role of the AhR during IVM can contribute to our understanding of the complexity of mammalian oocyte maturation and, in turn, provide fresh information on the xenobiotic-independent activity of the AhR.

2. MATERIALS AND METHODS

2.1. Reagents

Unless otherwise stated, all reagents were purchased from Sigma (St. Louis, MO, USA).

2.2. Cumulus-oocyte complexes collection

Bovine ovaries were collected from a slaughterhouse and transported within 2 hours to the laboratory in Dulbecco's phosphate balanced saline (PBS) supplemented with 100 000 IU

penicillin, 100 mg streptomycin and 250 µg amphotericin B per liter at a temperature of 36 °C.

COCs were retrieved by aspiration from mid-antral follicles (2-6 mm) and washed three times in TCM 199 supplemented with 0.4% BSA, 25 mM HEPES, and 10 µg/mL heparin.

Based on the number of layers of cumulus cells and ooplasm character, the COCs were graded into three classes namely A, B, and C. Class A oocytes were characterized with at least three complete layers of cumulus cells and uniform granulation of ooplasm; class B with one or two complete layers of cumulus cells and uniform granulation of ooplasm; class C as denuded oocytes with uniform granulation of ooplasm. Oocytes with heterogeneous/clustered cytoplasm were classified as degenerated independently from the number of layers of cumulus cells. Only Class A COCs were selected as suitable for IVM and used for the subsequent experiments as previously described [7].

2.3. *In vitro* maturation

Basic maturation medium (bMM) was TCM 199, supplemented with 0.68 mM L-glutamine, 25 mM $NaHCO_3$, 10% (v/v) fetal calf serum, 10 IU/mL pregnant mare's serum gonadotropin (PMSG), 5 IU/mL hCG (Intervet, Wiesbaden, Germany) and 1 µg/mL 17-ß-estradiol. Groups of 25-35 COCs were matured in 500 µL bMM for 24h (or different periods as described in experimental design) at 39 °C in a humid atmosphere of 5% CO_2 in air. At the end of the maturation period, oocyte morphology was assessed by observing cumulus expansion, the size of the perivitelline space and the presence of an intact oolemma.

2.4. Experimental design

Experiments consisted of at least 3 groups of COCs/treatment and were replicated at least three times.

Experiment I. The objective was to assess the effect of inducing the meiotic arrest on the level of CYP1A1 mRNA and protein in COCs. ERK1/2 phosphorylation status in treated and control COCs was also studied. Control COCs were cultured in bMM and compared to COCs supplemented with: i) 4 mM 6-dimethylaminopurine (6-DMAP) or 10 µM cycloheximide for 24h; ii) 4 mM 6-DMAP for 24h followed by 24h with bMM alone. A total of 1046 COCs were used, separated in groups according to the treatment. Concentrations of inhibitors were chosen based on literature data as reported by Lonergan et al. (1997) and stock solutions of 6-DMAP and cycloheximide were diluted in bMM.

Experiment II: The aim was to explore the relationship between AhR-mediated CYP1A1 expression and the EGFR-ERK1/2 signaling pathway during IVM. As endpoints we measured the relative abundance of CYP1A1 mRNA and protein, the phosphorylation level of ERK1/2, and the outcome–of oocyte maturation. Control COCs were compared to COCs supplemented with: i) 10 µM AG1478 for 24h; ii) 10 µM PD98059 for 3, 15 and 24h of culture; iii) 15h culture with bMM alone followed by 9h exposure to 10 µM PD98059. A total of 2026 COCs were used, separated in groups according to the treatment. Stock solutions of both PD98059 and AG1478 were prepared in DMSO and controls received vehicle alone. AG1478 dose was chose~~n~~ according to Albuz F (2009). PD98059 concentration was based on literature data on treatments of cumulus oocyte complexes in other species (Meinecke & Krischek, 2003; Gall et al., 2005; LaRosa & Downs, 2005; Zhang et al., 2006). The PD98059 concentration chosen for the present study in bovine COCs was selected based on the results of preliminary experiments (data not shown).

Experiment III: The aim was to further explore the molecular relationship between AhR- and EGFR-ERK1/2-pathway. Control COCs were compared to COCs exposed to 40 µM of the AhR-antagonist resveratrol during IVM, and the relative expression levels of CYP1A1 mRNA and protein, and the phosphorylation level of ERK1/2 were analyzed. A

total of 492 COCs were used, separated in groups according to the treatment. Resveratrol stock solution was diluted in ethanol and controls received vehicle alone. Resveratrol concentration was based on dose-response curve obtained in previous study as reported by Pocar et al. (2004).

2.5. Evaluation of oocyte nuclear morphology

The stage of nuclear maturation was assessed in a total of 814 oocytes, separated in groups of at least 20 COCs according to the treatment. Each treatment (with the corresponding control) was replicated at least three times. Nuclear morphology was analyzed by 1% lacmoid staining under a phase contrast microscope as previously described [30]. Oocytes were classified as immature (germinal vesicle and germinal vesicle breakdown stage), intermediate (metaphase I and anaphase I), and mature (telophase I and metaphase II). Oocytes showing multipolar meiotic spindles, irregular chromatin clumps or no chromatin were considered degenerated.

2.6. mRNA isolation and complementary DNA synthesis

Poly(A)$^+$RNA from pools of 30 COCs was isolated according to Pocar et al. [7] using a Dynabeads mRNA DIRECT kit (Deutsche Dynal, Hamburg, Germany). Samples were quantified using a NanoDrop spectrophotometer (Thermo Scientific, Rockford, IL, USA) and 50 ng/sample of mRNA were immediately used for reverse transcription with the Perkin Elmer PCR Core kit using 2.5 µmol random hexamers to get the widest array of cDNAs. RT reaction was carried out in a final volume of 20 µL at 25 °C for 10 min, 42 °C for 1h, followed by a denaturation step at 99 °C for 5 min.

2.7. Semi-quantitative PCR

Semi-quantitative PCR was performed to measure gene expression of *CYP1A1*. To normalize signals from different RNA samples, β-actin transcripts were co-amplified as an internal standard. The amplification reaction was stopped before leaving the exponential phase. Each PCR reaction was performed in a total volume of 30 µL containing, 1X PCR buffer, 1.5 mM $MgCl_2$, 0.2 mM dNTPs, 1U Taq DNA polymerase, 2 µL first-strand cDNA, 0.2 µM of the primer combination (forward: TCGGGCACATGCTGATGTTG; reverse: GCACAGATGACATTGGCCACTG) [7]. An initial denaturation step of 3 min at 94 °C was followed by 35 cycles of: 30 sec 94 °C, 30 sec 57 °C, 45 sec 72 °C and end step 5 min 72 °C. A water control was included to identify contamination. All samples were amplified with an intron-exon spanning primer pair to detect genomic DNA contamination. β-actin (forward: CCAAGGCCAACCGTGAGAAG, reverse: CCATCTCCTGCTTCGAAGTCC) was used as the reference gene for *CYP1A1*. PCR products were sequenced to verify their identity and homology to corresponding mRNA sequences in the EMBL databank.

One sample of 20 µL per reaction was loaded onto ethidium bromide stained 1.5% agarose gels in TAE buffer and visualized on a 312 nm UV-transilluminator. The image of each gel was digitalized with a CCD camera and the intensity of each band was quantified by densitometric analysis using BioProfil, LTF software. The relative amount of the mRNA of interest was calculated as a percentage of the intensity of the β-actin band for the corresponding sample. Experiments were replicated at least three times.

2.8. Electrophoresis and immunoblot analysis

Groups of 20 COCs were lysed using RIPA buffer with added proteinase and phosphatase inhibitors. Extracted proteins were quantified using Micro BCA™ Protein Assay Kit (Thermo Fisher Scientific, Inc., Waltham, MA, USA) and adjusted to a concentration of 0.5 mg/mL. Twenty µL of protein solution (10 µg) were mixed 1:1 with 2 × Laemmli

sample buffer and heated to 90 °C for 5 min, centrifuged at 13,000 rpm for 2 min and submitted to denaturing SDS-PAGE electrophoresis. Immunoblot analysis was done as described previously (Pocar et al., 2004). Briefly, membranes were primed with antibodies against CYP1A1 (Dianova, Hamburg, Germany) or anti-diphosphorylated ERK1/2 (M8159). Proteins of interest were detected with HRP-conjugated donkey anti-rabbit and goat anti-mouse IgG, respectively (Pierce Chemical Co., Rockford, USA) and visualized with the WestPico ECL detection system (Pierce Chemical Co.), according to the provided protocol. The membranes were stripped and re-probed with a monoclonal anti-β-actin antibody (A1978) as a loading control. Finally, individual band intensity was determined by peak areas determination with ChemiDoc documentation system (Lab-Works software 4.5—LTF). The relative amount of the protein of interest was calculated from the ratio of its densitometry value in reference to the densitometry value of its own β-ACTIN content. Experiments were replicated at least three times.

2.9. Statistical analysis

Data for *in vitro* culture were analyzed using a binary logistic regression. Controls were assumed as reference group. Experiments were replicated at least three times, and each replicate was fitted as a factor. The log likelihood ratio statistic was used to detect between treatment differences using the SPSS statistical package (SPSS Institute, Inc., Chicago, IL). Data for gene expression were assessed using t-test or ANOVA followed by Fisher's protected least significant difference test. In all cases the criterion for significance was set at $P \leq 0.05$.

3. RESULTS

3.1. Activation of phosphorylation cascades is required for AhR transcriptional activity during bovine oocyte IVM

The activity of the AhR in bovine cumulus-oocyte complexes was assessed after exposure for 24h to the broad-spectrum serine/threonine kinase inhibitor 6-DMAP or to the protein synthesis inhibitor cycloheximide, conditions that are well-known to induce meiotic arrest.

As shown in Table 1 both treatments maintained the oocytes at the immature stage for the entire period of culture. The exposure to 6-DMAP significantly downregulated CYP1A1 compared to control at both transcript and protein level (Fig 1A, B) and significantly downregulated the phosphorylation status of ERK1/2 (Fig 1B). Conversely, in cycloheximide treated COCs no effects were observed on CYP1A1 transcript expression (Fig 2A) and on the p-ERK1/2 phosphorylation status (Fig. 2B).

The effects of 6-DMAP were completely reversible. Culture of COCs for a second 24h in inhibitor-free medium allowed: i) retrieval of ERK1/2 phosphorylation level; ii) recovery of the oocytes' maturation capacity, with 71.7% of 6-DMAP-treated COCs reaching the metaphase II stage (Table 1); and iii) the recovery of CYP1A1 to transcript and protein levels comparable to control (Fig. 1).

These results strongly suggest a key role of phosphorylation cascades in triggering AhR transcriptional activity during bovine oocyte IVM.

3.2. EGFR-ERK1/2 signaling pathway participates in mediation of AhR activity during IVM

The potential relationship between AhR-mediated *CYP1A1* expression and the EGFR-ERK1/2 signaling during bovine oocyte maturation was explored by exposure to EGFR-erb1/4-ERK1/2 inhibitor and to a specific MEK inhibitor.

Incubation with EGFR inhibitor AG1478 significantly attenuated the expression of the AhR-induced CYP1A1 transcript and protein expression, together with reduced phosphorylation levels of ERK1/2 (Fig. 3). In addition, exposure to AG1478 affected oocyte maturation competence with a significant increase of oocytes at the intermediate stage at the end of the culture period compared to control (Table 2).

Exposure of COCs to the specific MEK inhibitor PD98059 significantly affected *CYP1A1* transcript expression (Fig. 4A), ERK1/2 phosphorylation (Fig. 4B) and oocyte maturation (Table 3). Interestingly, there was a time-dependent change in both *CYP1A1* mRNA expression and the phosphorylation status of ERK1/2. *CYP1A1* mRNA expression was downregulated at 3h and 15h of culture, followed by substantial upregulation at 24h. Concurrently, phosphorylation was virtually absent at 3h for both ERKs, partially restored for ERK2 at 15h, and fully restored for both ERKs at 24h.

To verify whether these recoveries depended on the gradual loss of activity of PD98059 in the maturation medium - as seen in other culture systems [31] - we exposed the COCs to PD98059 from 15h to the end of the culture. Under these conditions *CYP1A1* transcript expression was downregulated (Fig. 4A), and phosphorylation of both ERK1 and 2 was significantly reduced (Fig. 4B).

In parallel with the effects on *CYP1A1* and ERK1/2, there was a significant delay in the oocytes' ability to complete maturation (Table 3). All the PD98059 treated oocytes were able to resume meiosis (i.e. no immature), but after 24h of culture a significantly larger percentage than control remained in the metaphase stage I (intermediate). In agreement with the transient effects of PD98059 at molecular level on *CYP1A1* expression and ERK1/2 phosphorylation, another 12h of culture (i.e. total 36h) completely restored the oocytes' ability to reach the metaphase stage II (Table 3).

These data indicate a correlation between EGFR and post-EGFR ERK1/2 signaling activity and AhR-mediated *CYP1A1* induction during IVM possibly playing a role in the metaphase I to metaphase II transition.

3.3. EGFR-ERK1/2 signaling pathway acts upstream to AhR activation in bovine COCs

To gain insights into the role of EGFR-ERK1/2 signaling on AhR activation during oocyte maturation we exposed bovine COCs to the AhR antagonist resveratrol during IVM.

The exposure of COCs for 24h to resveratrol significantly downregulated the expression of CYP1A1 at both transcript and protein level, while no effects were observed on the phosphorylation status of ERK1/2 (Fig. 5). Resveratrol also significantly reduced the percentage of oocytes that reached the metaphase II stage, increasing the proportion of oocytes arrested in intermediate stages after 24 h of culture (Table 4).

Taken together, these data suggest that EGFR and post-EGFR ERK1/2 signaling constitute an upstream event in the AhR activation in bovine COCs during IVM.

4. DISCUSSION

The present study shows that during bovine oocyte maturation the AhR-mediated gene expression in COCs depends on EGFR and post-EGFR ERK1/2 signaling. To the best of our knowledge this is first time that cross-talk between the signaling pathways of AhR, EGFR and ERK1/2 has been observed in COCs, so a major role for this interaction is suggested for the correct progression of oocyte meiotic maturation.

Oocyte maturation is regulated not only by the gonadotropic hormones, but also by growth factors produced directly in the ovary. There is substantial evidence of a physiological role of the epidermal growth factor (EGF) in the release of mammalian oocytes from meiotic

arrest. These properties of EGF appear to be mediated through cumulus cells that have functional EGFR in fully grown antral follicles (review in [32]). The RAS-RAF-MEK-ERK1/2 pathway is the most important pathway in the biological response of the EGFR. In COCs EGFR-activated ERK1/2 interacts with over a hundred substrates involved in the regulation of transcriptional and post-transcriptional events leading to meiotic resumption and cumulus expansion [32, 33]. In the present study we found that in bovine COCs during IVM the EGFR and EGFR-mediated ERK1/2 signaling also significantly influenced the AhR transcriptional response.

In agreement with these observations, in various animal models TCDD intoxication or exogenous EGF administration induces similar severe biological effects, such as inhibition of palatal fusion [34], promotion of skin tumorigenesis [35] or premature tooth eruption, and loss of body and thymus weight [36, 37], suggesting that TCDD and EGF probably affect the same cellular target structures.

The observation that in COCs EGFR-mediated ERK1/2 phosphorylation is required for AhR-mediated gene expression is further in agreement with studies in cell lines, where AhR-mediated *CYP1A1* induction upon ligand binding was inhibited by specific block of ERK1/2 phosphorylation, together with reduced cellular effects [38, 39]. Yim et al. [40] observed that over-expression of constitutively active MEK1 enhanced the TCDD-initiated transactivation potential of the receptor, whereas over-expression of a dominant-negative variant of MEK1 or treatment with a MEK1 inhibitor reduced TCDD-dependent binding of the AhR to its cognate DNA motif in the *CYP1A1* gene promoter. Accordingly to our observation in COCs, in these cell lines *CYP1A1* expression was only partially inhibited by ERK1/2 inactivation, suggesting that the ERK pathway is only partially responsible for the induction of AhR activity and that complete AhR activation is likely to involve multiple signaling in phosphorylation cascades [38]. We are aware that the observation of blocking *CYP1A1* induction by PD98059 alone

cannot be confidently attributed to an ERK1/2-mediated mechanism. Indeed, PD98059 is a flavonoid and due to its chemical structure has been recognized as an equipotent AhR antagonist and inhibitor of MEK [41]. However, in our experimental model the PD98059 effects were very similar to those of AG1478, which is not an AhR antagonist. This overlapping pattern of effects strongly supports the hypothesis that the ERK1/2 signaling cascade might modulate the AhR activation in COCs during oocyte maturation.

Treatment of bovine COCs with specific AhR antagonists significantly impaired oocyte maturation, mirroring the effects observed here with the EGFR and MEK inhibitors [7], clearly suggesting a vital role of AhR/ERK cross-talk for the correct progression of meiotic resumption. This hypothesis closely lines up with the observation that ERK1/2 and AhR knock-out (AhRKO) mice share a similar ovarian phenotype. Specifically, when ERK1/2 was disrupted in mouse granulosa and cumulus cells, oocyte maturation, cumulus expansion and ovulation failed to occur in response to hCG [42]. Similarly, AhRKO ovaries show fewer ovulations than wild type mice, together with a lower capacity of AhRKO follicles to respond to gonadotropins [14, 43]. Interestingly, in the present study we observed that treatment with specific AhR antagonist resveratrol do not interfere with ERK1/2 phosphorylation status suggesting the initiation of EGFR and post-EGFR ERK1/2 signaling as an upstream event to AhR activation.

Recent studies indicate that AhR activation directly regulates the expression of EGF-like cytokines such as epiregulin (EREG [44, 45]) and amphiregulin (AREG [46]) in different cell type. Interestingly, oocyte maturation and cumulus expansion involve non-classical, prolonged activity of the EGFR pathway and it has been suggested that the physiological surge of LH requires local sustained EGFR activity not only to mediate but also to maintain its switch-like stimulation [47]. One may therefore speculate that an AhR/EGFR two-way cross-talk might be activated in bovine COCs during maturation. The stimulation of the

EGFR pathway would start the cascade of phosphorylations culminating in the activation of ERK1/2 which, in turn, would mediate an ill-defined step in the process of AhR activation, possibly auto-amplifying the expression of EGF-like peptides. These regulatory loop might be to some extent be involved in the specific prolonged activity of EGFR characteristic of oocyte maturation.

In line with this interpretation, it is worth noting that prolonged EGFR activity in the ovary is associated with unique, sustained upregulation of *PTGS2*, a gene essential for cumulus expansion [47]. Similarly, benzo(a)pyrene-mediated AhR activation results in induction of *PTGS2* expression in human placenta [48].

In conclusion, we report here for the first time a functional cross-talk between AhR and EGFR/ERK signaling pathways during oocyte maturation. Our results further support the evidence that constitutive activation of AhR in COCs is a normal, finely tuned physiological mechanism essential to sustain the oocyte's meiotic resumption.

These findings may prove valuable not only in basic science as regards a deeper understanding of the complex molecular mechanisms orchestrating oocyte maturation but also for reproductive biotechnologies in mammals, to improve their efficiency.

ACKNOWLEDGEMENTS

This research did not receive any specific grant from funding agencies in the public, commercial, or not-for-profit sectors.

DECLARATION OF INTEREST: none

REFERENCES

1. Eppig JJ. Coordination of nuclear and cytoplasmic oocyte maturation in eutherian mammals. Reproduction, fertility, and development 1996;8:485-9.

2. Watson AJ. Oocyte cytoplasmic maturation: a key mediator of oocyte and embryo developmental competence. Journal of animal science 2007;85:E1-3.
3. Zuccotti M, Merico V, Cecconi S, Redi CA, Garagna S. What does it take to make a developmentally competent mammalian egg? Human reproduction update 2011;17:525-40.
4. Canipari R, Cellini V, Cecconi S. The ovary feels fine when paracrine and autocrine networks cooperate with gonadotropins in the regulation of folliculogenesis. Current pharmaceutical design 2012;18:245-55.
5. Richards JS. Delivery of the oocyte from the follicle to the oviduct: a time of vulnerability. Ernst Schering Research Foundation workshop 2002:43-62.
6. Nestler D, Risch M, Fischer B, Pocar P. Regulation of aryl hydrocarbon receptor activity in porcine cumulus-oocyte complexes in physiological and toxicological conditions: the role of follicular fluid. Reproduction 2007;133:887-97.
7. Pocar P, Augustin R, Fischer B. Constitutive expression of CYP1A1 in bovine cumulus oocyte-complexes in vitro: mechanisms and biological implications. Endocrinology 2004;145:1594-601.
8. Nebert DW. Aryl hydrocarbon receptor (AHR): "pioneer member" of the basic-helix/loop/helix per-Arnt-sim (bHLH/PAS) family of "sensors" of foreign and endogenous signals. Prog Lipid Res 2017;67:38-57.
9. Denison MS, Nagy SR. Activation of the aryl hydrocarbon receptor by structurally diverse exogenous and endogenous chemicals. Annu Rev Pharmacol Toxicol 2003;43:309-34.
10. Swanson HI, Bradfield CA. The AH-receptor: genetics, structure and function. Pharmacogenetics 1993;3:213-30.
11. Bock KW, Kohle C. Ah receptor: dioxin-mediated toxic responses as hints to deregulated physiologic functions. Biochem Pharmacol 2006;72:393-404.
12. Nebert DW, Roe AL, Dieter MZ, Solis WA, Yang Y, Dalton TP. Role of the aromatic hydrocarbon receptor and [Ah] gene battery in the oxidative stress response, cell cycle control, and apoptosis. Biochem Pharmacol 2000;59:65-85.
13. Benedict JC, Lin TM, Loeffler IK, Peterson RE, Flaws JA. Physiological role of the aryl hydrocarbon receptor in mouse ovary development. Toxicol Sci 2000;56:382-8.
14. Benedict JC, Miller KP, Lin TM, Greenfeld C, Babus JK, Peterson RE, et al. Aryl hydrocarbon receptor regulates growth, but not atresia, of mouse preantral and antral follicles. Biol Reprod 2003;68:1511-7.

15. Fernandez-Salguero P, Pineau T, Hilbert DM, McPhail T, Lee SS, Kimura S, et al. Immune system impairment and hepatic fibrosis in mice lacking the dioxin-binding Ah receptor. Science 1995;268:722-6.
16. Lahvis GP, Lindell SL, Thomas RS, McCuskey RS, Murphy C, Glover E, et al. Portosystemic shunting and persistent fetal vascular structures in aryl hydrocarbon receptor-deficient mice. Proc Natl Acad Sci U S A 2000;97:10442-7.
17. Adachi J, Mori Y, Matsui S, Takigami H, Fujino J, Kitagawa H, et al. Indirubin and indigo are potent aryl hydrocarbon receptor ligands present in human urine. J Biol Chem 2001;276:31475-8.
18. Nguyen LP, Bradfield CA. The search for endogenous activators of the aryl hydrocarbon receptor. Chem Res Toxicol 2008;21:102-16.
19. Soshilov AA, Denison MS. Ligand promiscuity of aryl hydrocarbon receptor agonists and antagonists revealed by site-directed mutagenesis. Mol Cell Biol 2014;34:1707-19.
20. Beischlag TV, Luis Morales J, Hollingshead BD, Perdew GH. The aryl hydrocarbon receptor complex and the control of gene expression. Crit Rev Eukaryot Gene Expr 2008;18:207-50.
21. Frericks M, Meissner M, Esser C. Microarray analysis of the AHR system: tissue-specific flexibility in signal and target genes. Toxicol Appl Pharmacol 2007;220:320-32.
22. Goodale BC, Tilton SC, Corvi MM, Wilson GR, Janszen DB, Anderson KA, et al. Structurally distinct polycyclic aromatic hydrocarbons induce differential transcriptional responses in developing zebrafish. Toxicol Appl Pharmacol 2013;272:656-70.
23. Hruba E, Vondracek J, Libalova H, Topinka J, Bryja V, Soucek K, et al. Gene expression changes in human prostate carcinoma cells exposed to genotoxic and nongenotoxic aryl hydrocarbon receptor ligands. Toxicol Lett 2011;206:178-88.
24. Puga A, Ma C, Marlowe JL. The aryl hydrocarbon receptor cross-talks with multiple signal transduction pathways. Biochem Pharmacol 2009;77:713-22.
25. Wee P, Wang Z. Epidermal Growth Factor Receptor Cell Proliferation Signaling Pathways. Cancers (Basel) 2017;9.
26. Verlhac MH, de Pennart H, Maro B, Cobb MH, Clarke HJ. MAP kinase becomes stably activated at metaphase and is associated with microtubule-organizing centers during meiotic maturation of mouse oocytes. Dev Biol 1993;158:330-40.

27. Verlhac MH, Kubiak JZ, Clarke HJ, Maro B. Microtubule and chromatin behavior follow MAP kinase activity but not MPF activity during meiosis in mouse oocytes. Development 1994;120:1017-25.
28. Ashkenazi H, Cao X, Motola S, Popliker M, Conti M, Tsafriri A. Epidermal growth factor family members: endogenous mediators of the ovulatory response. Endocrinology 2005;146:77-84.
29. Tong C, Fan HY, Chen DY, Song XF, Schatten H, Sun QY. Effects of MEK inhibitor U0126 on meiotic progression in mouse oocytes: microtuble organization, asymmetric division and metaphase II arrest. Cell Res 2003;13:375-83.
30. Luciano AM, Pocar P, Milanesi E, Modina S, Rieger D, Lauria A, et al. Effect of different levels of intracellular cAMP on the in vitro maturation of cattle oocytes and their subsequent development following in vitro fertilization. Mol Reprod Dev 1999;54:86-91.
31. Zhang WL, Huitorel P, Geneviere AM, Chiri S, Ciapa B. Inactivation of MAPK in mature oocytes triggers progression into mitosis via a Ca2+ -dependent pathway but without completion of S phase. J Cell Sci 2006;119:3491-501.
32. Prochazka R, Blaha M, Nemcova L. Significance of epidermal growth factor receptor signaling for acquisition of meiotic and developmental competence in mammalian oocytes. Biol Reprod 2017;97:537-49.
33. Shimada M, Hernandez-Gonzalez I, Gonzalez-Robayna I, Richards JS. Paracrine and autocrine regulation of epidermal growth factor-like factors in cumulus oocyte complexes and granulosa cells: key roles for prostaglandin synthase 2 and progesterone receptor. Mol Endocrinol 2006;20:1352-65.
34. Yamamoto T, Cui XM, Shuler CF. Role of ERK1/2 signaling during EGF-induced inhibition of palatal fusion. Dev Biol 2003;260:512-21.
35. Rose SP, Stahn R, Passovoy DS, Herschman H. Epidermal growth factor enhancement of skin tumor induction in mice. Experientia 1976;32:913-5.
36. Haarmann-Stemmann T, Bothe H, Abel J. Growth factors, cytokines and their receptors as downstream targets of arylhydrocarbon receptor (AhR) signaling pathways. Biochem Pharmacol 2009;77:508-20.
37. Madhukar BV, Brewster DW, Matsumura F. Effects of in vivo-administered 2,3,7,8-tetrachlorodibenzo-p-dioxin on receptor binding of epidermal growth factor in the hepatic plasma membrane of rat, guinea pig, mouse, and hamster. Proc Natl Acad Sci U S A 1984;81:7407-11.

38. Tan Z, Chang X, Puga A, Xia Y. Activation of mitogen-activated protein kinases (MAPKs) by aromatic hydrocarbons: role in the regulation of aryl hydrocarbon receptor (AHR) function. Biochem Pharmacol 2002;64:771-80.
39. Vazquez-Gomez G, Rocha-Zavaleta L, Rodriguez-Sosa M, Petrosyan P, Rubio-Lightbourn J. Benzo[a]pyrene activates an AhR/Src/ERK axis that contributes to CYP1A1 induction and stable DNA adducts formation in lung cells. Toxicol Lett 2018;289:54-62.
40. Yim S, Oh M, Choi SM, Park H. Inhibition of the MEK-1/p42 MAP kinase reduces aryl hydrocarbon receptor-DNA interactions. Biochem Biophys Res Commun 2004;322:9-16.
41. Reiners JJ, Jr., Lee JY, Clift RE, Dudley DT, Myrand SP. PD98059 is an equipotent antagonist of the aryl hydrocarbon receptor and inhibitor of mitogen-activated protein kinase kinase. Molecular pharmacology 1998;53:438-45.
42. Fan HY, Liu Z, Shimada M, Sterneck E, Johnson PF, Hedrick SM, et al. MAPK3/1 (ERK1/2) in ovarian granulosa cells are essential for female fertility. Science 2009;324:938-41.
43. Barnett KR, Tomic D, Gupta RK, Babus JK, Roby KF, Terranova PF, et al. The aryl hydrocarbon receptor is required for normal gonadotropin responsiveness in the mouse ovary. Toxicol Appl Pharmacol 2007;223:66-72.
44. John K, Lahoti TS, Wagner K, Hughes JM, Perdew GH. The Ah receptor regulates growth factor expression in head and neck squamous cell carcinoma cell lines. Mol Carcinog 2014;53:765-76.
45. Patel RD, Kim DJ, Peters JM, Perdew GH. The aryl hydrocarbon receptor directly regulates expression of the potent mitogen epiregulin. Toxicol Sci 2006;89:75-82.
46. Choi SS, Miller MA, Harper PA. In utero exposure to 2,3,7,8-tetrachlorodibenzo-p-dioxin induces amphiregulin gene expression in the developing mouse ureter. Toxicol Sci 2006;94:163-74.
47. Reizel Y, Elbaz J, Dekel N. Sustained activity of the EGF receptor is an absolute requisite for LH-induced oocyte maturation and cumulus expansion. Mol Endocrinol 2010;24:402-11.
48. Palatnik A, Xin H, Su EJ. Dichotomous effects of aryl hydrocarbon receptor (AHR) activation on human fetoplacental endothelial cell function. Placenta 2016;44:61-8.

FIGURE LEGENDS

Fig. 1. A) Effect of exposure to 6-dymethylaminopurine (6-DMAP) in bovine COCs during IVM. Ctrl: 24h culture with bMM alone; 6-DMAP: 24h culture with 4 mM 6-DMAP; 6-DMAP + ctrl: 24h with 4 mM 6-DMAP followed by 24h with bMM alone. A) Effect of exposure to 6-DMAP on *CYP1A1* transcript expression. The C*YP1A1*/*β-ACTIN* densitometric ratio is shown (mean ± SE). Asterisks indicate significant differences between columns ($p \leq 0.05$). B) Representative immunoblots for CYP1A1, p-ERK1/2 and β-ACTIN proteins on solubilized extracts corresponding to 20 COCs. The CYP1A1/β-ACTIN and p-ERKs/β-ACTIN densitometric ratio is shown. Data are expressed as percentage to control (mean ± SE). Asterisks indicate significant differences between columns ($p \leq 0.05$).

Fig. 2. Effect of exposure to cycloheximide in bovine COCs during IVM. Ctrl: 24h culture with bMM alone; cycloheximide: 24h culture with 10 μM cycloheximide. A) Effect of exposure to cycloheximide on *CYP1A1* transcript expression. The C*YP1A1*/*β-ACTIN* densitometric ratio is shown (mean ± SE). Asterisks indicate significant differences between columns ($p \leq 0.05$). B) Representative immunoblots for p-ERK1/2 and β-ACTIN proteins on solubilized extracts corresponding to 20 COCs. The p-ERKs/β-ACTIN densitometric ratio is shown. Data are expressed as percentage to control (mean ± SE). Asterisks indicate significant differences between columns ($p \leq 0.05$).

Fig. 3. Effect of exposure to the selective EGFR inhibitor AG1478 in bovine COCs during IVM. COCs were harvested at 24h of culture with bMM alone (ctrl) or supplemented with AG1478 (10 μM). A) Effect of exposure to AG1478 on *CYP1A1* transcript and protein expression. The C*YP1A1*/*β-ACTIN* densitometric ratio is shown (mean ± SE). The asterisk

indicates a significant difference between columns ($p \leq 0.05$); B) Representative immunoblots for CYP1A1, p-ERK1/2 and β-ACTIN proteins on solubilized extracts corresponding to 20 COCs. The CYP1A1/β-ACTIN and p-ERKs/β-ACTIN densitometric ratio is shown. Data are expressed as percentage to control (mean ± SE). Asterisks indicate significant differences between columns ($p \leq 0.05$).

Fig. 4. Effect of exposure to the selective MEK inhibitor PD98059 in bovine COCs at different times during IVM. COCs were harvested at 3, 15 and 24h of culture with bMM alone (ctrl) or supplemented with 10 μM PD98059; PD98059 15-24h corresponds to 15h treatment with bMM alone followed by 9h exposure to 10 μM PD98059. A) Effect of exposure to PD98059 on *CYP1A1* transcript expression. The C*YP1A1/β-ACTIN* densitometric ratio is shown (mean ± SE). Asterisks indicate significant differences between columns ($p \leq 0.05$); B) Representative immunoblots for p-ERK1/2 and β-ACTIN proteins on solubilized extracts corresponding to 20 COCs. The p-ERKs/β-ACTIN densitometric ratio is shown. Data are expressed as percentage to control (mean ± SE). Asterisks indicate significant differences between columns ($p \leq 0.05$).

Fig. 5. Effect of exposure to the AhR antagonist resveratrol in bovine COCs during IVM. COCs were harvested at 24h of culture with bMM alone (ctrl) or supplemented with 40 μM resveratrol. A) Effect of exposure to resveratrol on *CYP1A1* transcript expression. The C*YP1A1/β-ACTIN* densitometric ratio is shown (mean ± SE). The asterisk indicates a significant difference between columns ($p \leq 0.05$); B) Representative immunoblots for CYP1A1, p-ERK1/2 and β-ACTIN proteins on solubilized extracts corresponding to 20 COCs. The CYP1A1/β-ACTIN and p-ERKs/β-ACTIN densitometric ratio is shown. Data are

582 expressed as percentage to control (mean ± SE). Asterisks indicate significant differences
583 between columns ($p \leq 0.05$).
584
585

Table 1

Table 1. Effects of exposure to 6-dymethylaminopurine (6-DMAP) or cycloheximide on bovine oocyte *in vitro* maturation

Treatment	No. of COCs[*]	Immature[**] (%)	Intermediate[**] (%)	Matured[**] (%)	Degenerated[**] (%)
Control	75	2.1[b]	18.7[b]	73.5[b]	5.5
Cycloheximide	63	96.9[a]	0.0[a]	0.0[a]	3.0
6–DMAP 24h	65	92.5[a]	0.0[a]	0.0[a]	7.5
6-DMAP 24h + control 24 h	63	6.0[b]	19.8[b]	71.7[b]	4.8

[*]Total number of oocytes allocated for each treatment (three replicates/treatment).

[**] Categorical culture data are expressed as mean percentages of oocytes at immature, intermediate, matured and degenerated status of the total number of oocytes.

[a,b] Different superscripts in the same column indicate significant differences ($P \leq 0.05$). Control was taken as reference.

Table 2. Effects of AG1478 on bovine oocyte *in vitro* maturation

Treatment	No. of COCs*	Immature** (%)	Intermediate** (%)	Matured** (%)	Degenerated (%)
Control	75	0.0	14.0[a]	82.2[a]	3.4
AG1478	65	1.7	53.4[b]	44.9[b]	0.0

*Total number of oocytes allocated for each treatment (three replicates/treatment).

** Categorical culture data are expressed as mean percentages of oocytes at germinal vesicle and germinal vesicle breakdown, metaphase I, metaphase II, and degenerated status of the total number of oocytes.

[a,b] Different superscripts in the same column indicate significant differences ($P \leq 0.05$). Control was taken as reference.

Table 3. Time-dependent effects of PD98059 on bovine oocyte *in vitro* maturation

Treatment	No. of COCs[*]	Immature[**] (%)	Intermediate[**] (%)	Matured[**] (%)	Degenerated[**] (%)
24 h ctrl	63	0.0	11.3[a]	84.7[a]	4.0
24 h PD98059	65	0.0	28.0[b]	68.0[b]	4.0
36 h ctrl	67	0.0	13.4	85.1	1.5
36 h PD98059	71	0.0	15.5	81.7	2.8

[*]Total number of oocytes allocated for each treatment (three replicates/treatment).

[**] Categorical culture data are expressed as mean percentages of oocytes at immature, intermediate, matured and degenerated status of the total number of oocytes.

[a,b] Different superscripts in the same column indicate significant differences ($P \leq 0.05$). Control was taken as reference.

Table 4. Effects of Resveratrol on bovine oocyte *in vitro* maturation

Treatment	No. of COCs*	Immature** (%)	Intermediate** (%)	Matured** (%)	Degenerated** (%)
Control	65	0.0	13.7[a]	84.5[b]	1.8
Resveratrol	67	6.5	52.3[b]	37.8[b]	3.4

*Total number of oocytes allocated for each treatment (three replicates/treatment).

** Categorical culture data are expressed as mean percentages of oocytes at germinal vesicle and germinal vesicle breakdown, metaphase I, metaphase II, and degenerated status of the total number of oocytes.

[a,b] Different superscripts in the same column indicate significant differences ($P \leq 0.05$). Control was taken as reference.

Figure 1

A

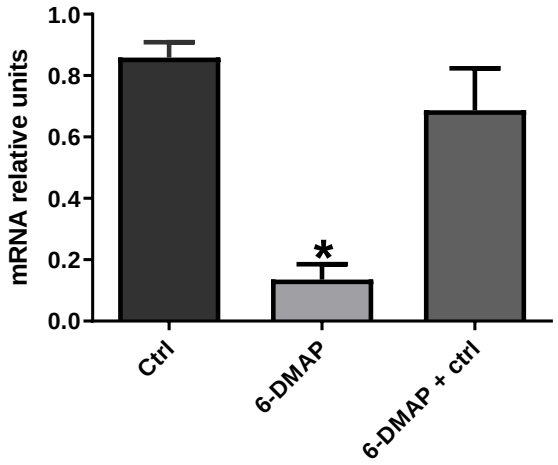
mRNA relative units
1.0
0.8
0.6
0.4
0.2
0.0
*
Ctrl
6-DMAP
6-DMAP + ctrl

B

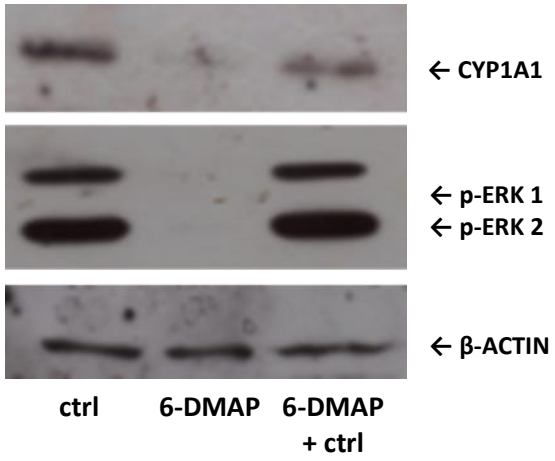
← CYP1A1
← p-ERK 1
← p-ERK 2
← β-ACTIN
ctrl
6-DMAP
6-DMAP + ctrl

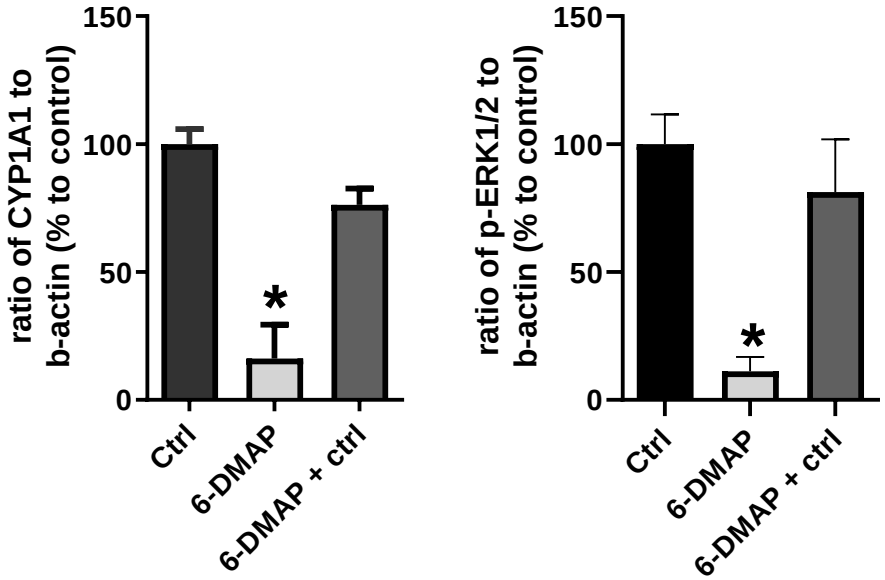
ratio of CYP1A1 to b-actin (% to control)
150
100
50
0
*
Ctrl
6-DMAP
6-DMAP + ctrl
ratio of p-ERK1/2 to b-actin (% to control)
150
100
50
0
*
Ctrl
6-DMAP
6-DMAP + ctrl

Figure 2

A

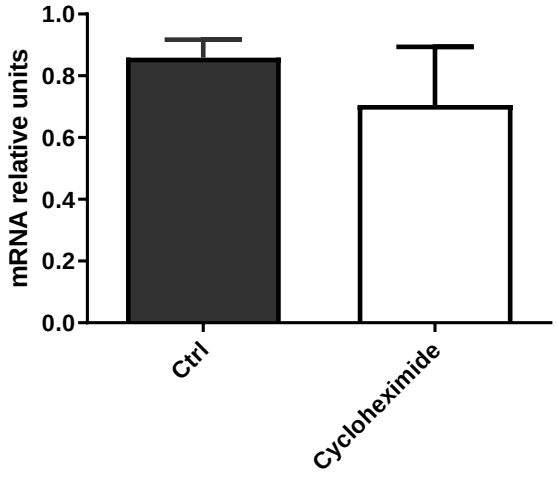
mRNA relative units
1.0
0.8
0.6
0.4
0.2
0.0
Ctrl
Cycloheximide

B

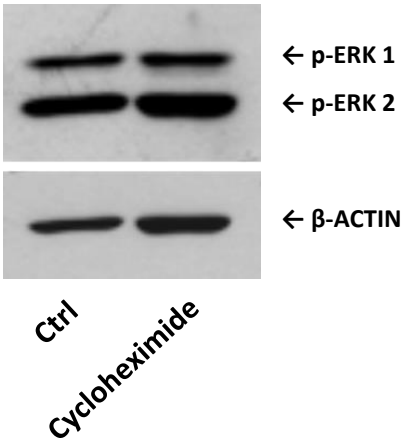
← p-ERK 1
← p-ERK 2
← β-ACTIN
Ctrl
Cycloheximide

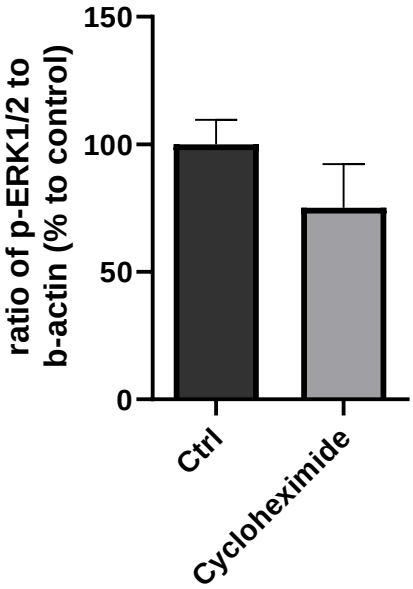
ratio of p-ERK1/2 to b-actin (% to control)
150
100
50
0
Ctrl
Cycloheximide

Figure 3

A

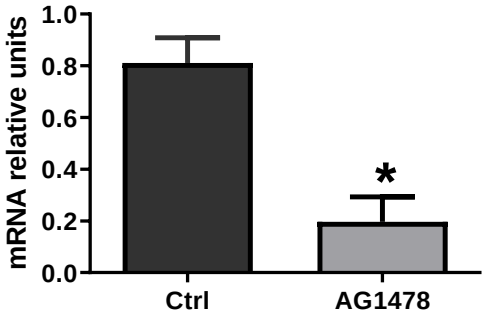
mRNA relative units
1.0
0.8
0.6
0.4
0.2
0.0
*
Ctrl
AG1478

B

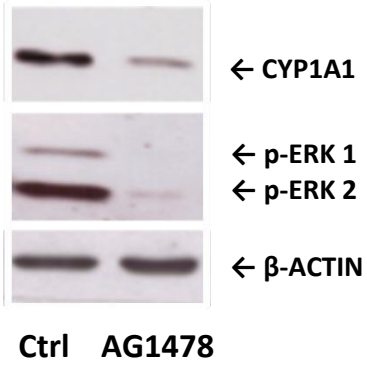
← CYP1A1
← p-ERK 1
← p-ERK 2
← β-ACTIN
Ctrl AG1478

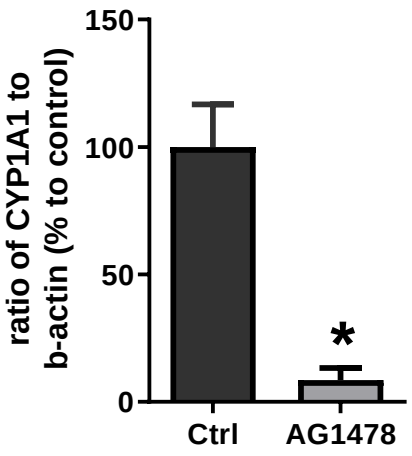
ratio of CYP1A1 to b-actin (% to control)
150
100
50
0
*
Ctrl
AG1478

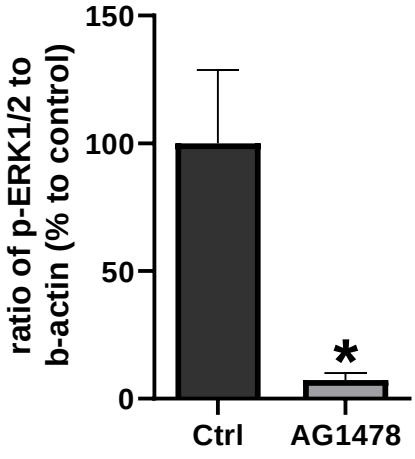
ratio of p-ERK1/2 to b-actin (% to control)
150
100
50
0
*
Ctrl
AG1478

Figure 4

A

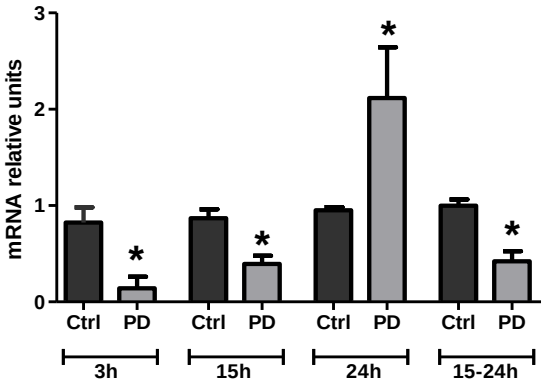
mRNA relative units
3
2
1
0
*
*
*
*
Ctrl PD Ctrl PD Ctrl PD Ctrl PD
3h
15h
24h
15-24h

B

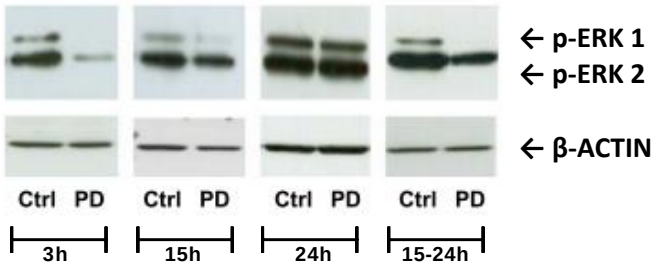
← p-ERK 1
← p-ERK 2
← β-ACTIN
Ctrl PD Ctrl PD Ctrl PD Ctrl PD
3h
15h
24h
15-24h

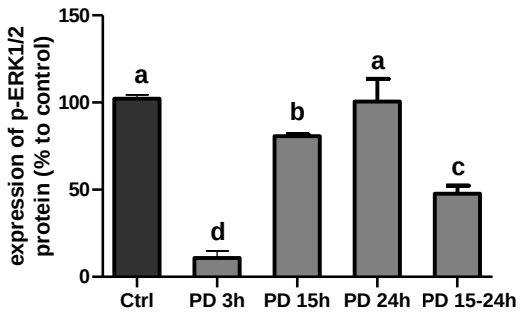
expression of p-ERK1/2 protein (% to control)
150
100
50
0
a
d
b
a
c
Ctrl
PD 3h
PD 15h
PD 24h
PD 15-24h

Figure 5

A

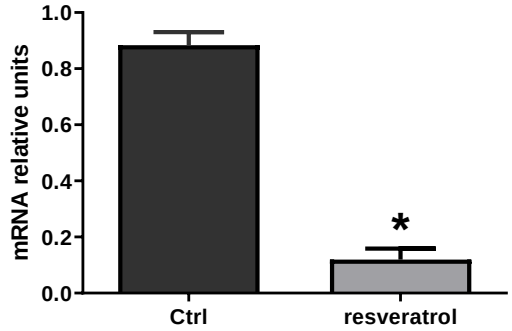
mRNA relative units
1.0
0.8
0.6
0.4
0.2
0.0
*
Ctrl
resveratrol

B

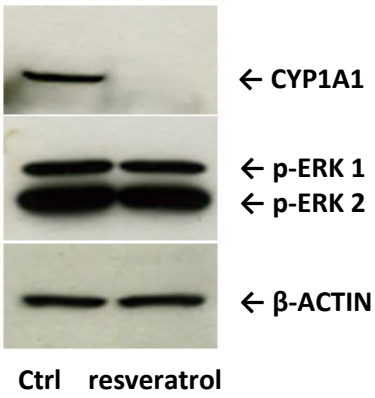
← CYP1A1
← p-ERK 1
← p-ERK 2
← β-ACTIN
Ctrl resveratrol

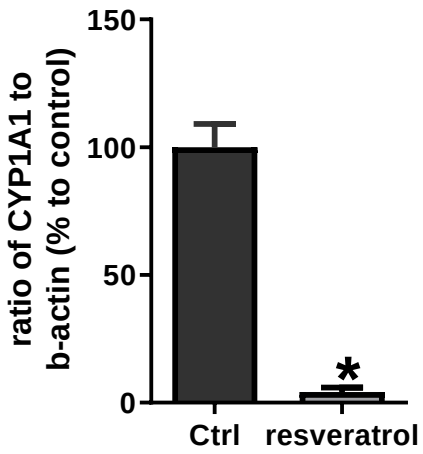
ratio of CYP1A1 to b-actin (% to control)
150
100
50
0
*
Ctrl resveratrol

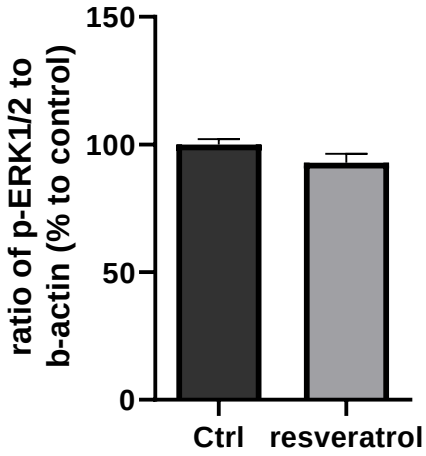
ratio of p-ERK1/2 to b-actin (% to control)
150
100
50
0
Ctrl resveratrol